

# Aerosil in Solid-state Buccal Film for Improved and Sustained Delivery of Valsartan: Molecular Docking Studies



R. Swain,<sup>a</sup> S. Nandi,<sup>a</sup> P. Bardhan,<sup>a</sup> S. S. Swain,<sup>b</sup> S. Mohapatra,<sup>a</sup> and S. Mallick<sup>a,\*</sup>

<sup>a</sup>Department of Pharmaceutics, School of Pharmaceutical Sciences, Siksha 'O' Anusandhan (Deemed to be University), Bhubaneswar-751003, Odisha, India

<sup>b</sup>Division of Microbiology & NCDs, ICMR-Regional Medical Research Centre, Chandrasekharapur, Bhubaneswar-751023

doi: <https://doi.org/10.15255/CABEQ.2022.2108>

Original scientific paper  
Received: June 18, 2022  
Accepted: March 2, 2023

To overcome low oral bioavailability and short biological half-life, improved and sustained buccal delivery of valsartan has been proposed. Valsartan film with colloidal silicon dioxide has been prepared using HPMC as mucoadhesive polymer matrix by casting and solvent evaporation method. Valsartan and Aerosil might have been interacted by hydrogen bond formation between adsorbed water and silanol of SiO<sub>2</sub>. *In vitro* drug release and *ex vivo* buccal permeation increased with the increase of Aerosil in the film. The formulation of valsartan to Aerosil at 1:0.02 ratio exhibited a sustained type of release and permeation of 80 and 70 %, respectively, in 8 h of study in simulated physiological fluid (pH 6.8). Molecular docking study revealed a stable configuration with favourable score of  $-2.15 \text{ kcal mol}^{-1}$  of the Aerosil incorporated valsartan buccal film. In conclusion, Aerosil incorporated hydrogel forming buccal film could be used for improved and sustained delivery of valsartan.

## Keywords

Aerosil 200, sustained permeation, valsartan, buccal film

## Introduction

Valsartan (VAL), an angiotensin II receptor antagonist relaxes blood vessels and improves blood flow for the control of hypertension.<sup>1</sup> It is a non-peptide tetrazole derivative with poor water solubility, inadequate gastrointestinal tract permeability, and high faecal elimination (86 %), resulting in low oral bioavailability of about 23 %.<sup>1</sup> VAL has teratogenic potential owing to adverse reactions, and should be discontinued orally in pregnancy. There is also a possibility of developing acute renal failure in patients with renal artery stenosis upon prolonged oral use in conventional form.<sup>2</sup>

Solid dispersion, liquisolid compact, self-microemulsifying drug administration, and supercritical antisolvent techniques have been reported for improving drug solubility and oral bioavailability.<sup>3–7</sup> The researchers have shown burst release of VAL with the increase in peak plasma concentration ( $C_{\text{max}}$ ) 4- to 7-fold compared to pure drug, and decrease in  $T_{\text{max}}$  to about 30 min. This may be sufficiently dangerous for exhibiting adverse drug reac-

tions. The pH-dependent drug release has been reported in another study of the developed valsartan hydrogel system.<sup>8</sup> The onset time *in vivo* may be delayed more than 3 h after oral administration (2 h residence in gastric region of pH 1.2 giving less than 10 % release, whereas, about 20 % release in 3<sup>rd</sup> h in the intestinal region of pH 7.4).

Aerosil 200, the commercially available fumed silicon dioxide (SiO<sub>2</sub>) of specific surface area 200 m<sup>2</sup> g<sup>-1</sup>, could be the promising carrier for increasing drug solubility because of the presence of siloxane and silanol groups on their large surface area.<sup>9</sup>

The buccal drug delivery system emphasizes drug administration through the mucosal membrane lining of the buccal cavity.<sup>10</sup> Drugs are absorbed from the oral mucosa, and transported through the jugular vein into the systemic circulation bypassing first pass metabolism of drug. Mucoadhesive HPMC film-type delivery systems may be more prominent and convenient for sustained buccal drug delivery by providing rapid onset of action.<sup>11,12</sup> Being a small molecule, valsartan will be the suitable drug candidate for buccal delivery for possible improvement of bioavailability compared to conventional oral delivery. The objective of the current research was to

\*Corresponding author: E-mail: [profsmallick@gmail.com](mailto:profsmallick@gmail.com)  
[subratamallick@soa.ac.in](mailto:subratamallick@soa.ac.in)

formulate Aerosil-incorporated HPMC matrix film for achieving improved and sustained buccal permeation of valsartan. Hydrogel forming HPMC can play a role in mucoadhesion, resulting in prolonged residence of film on the buccal tissue for probable effective sustained release of drug.<sup>13</sup>

## Material and methods

Valsartan was received as gift sample from Novartis (Mumbai, India). Hydroxypropyl methylcellulose (HPMC K 100M), Triethanolamine and Aerosil 200 (Specific surface area: 200 m<sup>2</sup> g<sup>-1</sup>) were purchased from HIMEDIA (Mumbai, India). All other reagents were of analytical grade.

### Preparation of valsartan buccal film

The casting and solvent evaporation method was used to formulate the film. Aerosil 200 was added in distilled water (300 µg mL<sup>-1</sup>) with overnight continuous magnetic stirring to prepare homogeneous dispersion. HPMC was soaked in a small amount of ice cool water for a few hours. The swelled HPMC gel was stirred magnetically for 3 hour, and stirring further continued after addition of an aliquot of Aerosil dispersion as per formulation given in Table 1. To that, VAL and triethanolamine mixture was added and agitated for about 2 h. The prepared hydrogel mixture was poured slowly into a casting plate (Tarsons, diameter: 90 mm), and left in an incubator for controlled drying at 40 °C for 24 h until a constant weight was obtained. A digital micrometre (Mitutoyo, Japan) was used to measure the thickness of film. Folding endurance (FE) was measured by folding a piece of film up to 200 times in the same position or until it was broken. The pH of the film surface was determined by immersing the glass electrode of a pH metre into the hydrated area of the film formulation.

### FTIR

The prepared films and the pure valsartan were scanned for IR transmission spectra to observe drug-excipient interactions, if any. The scans were

done in the 4000–400 cm<sup>-1</sup> range, with an average of 80 scans at a resolution of 4 cm<sup>-1</sup>. In the FTIR spectrophotometer (JASCO FT/IR 4600), the samples were put on a diamond ATR (JASCO ATR PRO ONE) crystal.

### DSC

Differential scanning calorimeter (DSC-1, Mettler Toledo, Switzerland) was used to evaluate the thermal properties of the film. The study was performed at 30–300 °C, varying at the rate of +10 °C, under 20.0 mL min<sup>-1</sup> nitrogen flow.

### XRD

X-ray powder crystallography (Rigaku Ultima IV) of the pure valsartan sample and the film formulations was carried out at a voltage of 40 kV and current flow of 15 mA. A scan rate of 1° min<sup>-1</sup> was maintained in the 2θ range of 5–70°. The source anode of the X-ray was Cu.

### SEM

Surface morphology of valsartan pure crystal and the films was studied with the help of a scanning electron microscope (ZEISS, EVO 18). A platinum sputter coat was applied prior to scanning the samples in SEM, and the surface morphology was examined at 1000–25000 times magnification using a 20 kV accelerated voltage at room temperature.

### In vitro drug release study

Using a USP type-II dissolution apparatus, the produced films were glued to a glass slide using cyanoacrylate adhesive, and completely immersed in 200 mL phosphate buffer saline (pH 6.8) in the dissolution vessel (Dissolution Tester USP, Electrolab TDT06L, India). The bath temperature was set at 34±0.2 °C, and the rotational speed was set to 50 rpm. To mimic the physiological temperature at the buccal surface, *in vitro* release test and permeation test were carried out at 34.0 ± 2 °C<sup>14</sup> up to 8 h. Sample of 10 mL was withdrawn at predetermined time interval using syringe driven filter (0.45 mm)

Table 1 – Formulation and physicochemical properties of valsartan film for buccal delivery

Film code	HPMC K100M (mg)	VAL: Aerosil ratio (wt/wt)	Triethanolamine (%)	Thickness (µm) mean ± sd; n=3	Surface pH	Folding endurance
VA0	1000	Aerosil -nill	15	199 ± 11.2	7.4	>200
VA1	1000	1:2·10 <sup>-2</sup>	15	224 ± 10.5	7.3	>200
VA2	1000	1:10 <sup>-2</sup>	15	220 ± 14.1	7.5	>200
VA3	1000	1:10 <sup>-3</sup>	15	189 ± 15.2	7.6	>200

for determination of cumulative drug release spectrophotometrically (JASCO, V-630 Spectrophotometer). Fresh dissolution medium was used to replenish the receptor medium.

### Ex vivo permeation study

Fresh chicken buccal mucosa was collected from the local butcher within 1 hour of its sacrifice for *ex vivo* permeation experiment. Another layer of dialysis membrane (Himedia Dialysis Membrane-150, LA401, molecular weight cut off 12000–14000) was attached to the buccal membrane for retaining colloidal SiO<sub>2</sub> particles of Aerosil. Proper size cut and accurately weighed film was placed on the buccal membrane over the dialysis membrane, and modified Franz diffusion cell was used for buccal mucosal permeation study. Phosphate buffer solution (PBS) of pH 6.8 (200 mL) was filled in the chamber for the study at 34±0.2 °C. Sample solutions of 10 mL volume were withdrawn at predetermined time intervals and analysed spectrophotometrically to obtain drug concentration. The steady-state flux ( $J_s$ ) was calculated from the slope obtained from the linear region using the amount permeation per cm<sup>2</sup> versus time plot. The permeability coefficient ( $P_{\text{film}}$ ) in cm min<sup>-1</sup> was determined by dividing steady-state flux with the concentration ( $C$ ) of valsartan in the film.<sup>15,16</sup>

$$P_{\text{film}} = J_s/C \quad (1)$$

### Kinetics

Both the *in vitro* drug release and *ex vivo* permeation data were applied with the Korsmeyer-Peppas model and Peppas-Sahlin model for determining drug release and permeation mechanism.<sup>16,17–19</sup> Based on Ficks's law of diffusion, Higuchi developed drug release kinetics as the linear relationship of cumulative percent drug release vs. square root of time plot.<sup>20</sup> Korsmeyer-Peppas law describes a simple and empirical equation using time-dependent power law in distinguishing the Fickian (diffusion controlled) and non-Fickian (anomalous transport) from the same equation.<sup>14,21</sup>

Korsmeyer-Peppas model:

$$C_t/C_\infty = Kt^n \quad (2)$$

$C_t/C_\infty$  – fraction of drug release/permeation of drug at time  $t$ ;  $K$  – Peppas release/permeation rate constant;  $n$  – release/permeation exponent

Peppas Sahlin model:<sup>22</sup>

$$M_t/M_\infty = K_1 t^m + K_2 t^{2m} \quad (3)$$

where  $M_t/M_\infty$  – fraction dissolved, %;  $K_1$  – constant related to the Fickian kinetics;  $K_2$  – constant related to Case II relaxation kinetics;  $m$  – diffusional exponent.

### Molecular docking study

The computational research was carried out on a Linux-Ubuntu 16.04 LTS system. The three-dimensional chemical structure of HPMC, silicon dioxide, and VAL were saved in .pdb file format after structural optimisation with Avogadro software. For the molecular docking investigation, AutoDock 4.2 software was utilised, followed by default settings with a user-defined grid box.<sup>16</sup> The molecular interactions of single and double docking complexes were then studied using BIOVIA DSV.<sup>23</sup>

## Results and discussion

### Physical properties

All of the film formulations were found to have uniform thickness ranging from 189 – 224 μm. Films showed a high folding endurance (>200), as well as sufficient strength and flexibility without becoming fragile. The pH of the film surface was found in the range of 7.3 and 7.6, which is thought to be safe for mucosal application. Film formulation with physical characteristics is presented in Table 1.

### FTIR

Samples of VAL, Aerosil, and film formulation were subjected to spectroscopic analysis and their spectra are shown in Fig. 1a. The IR spectrum of valsartan showed characteristic peaks at 2963, 1733, 1603, 1465 cm<sup>-1</sup> indicating the presence of C–H stretching, carboxyl carbonyl, amide carbonyl, C=C aromatic group, respectively.<sup>3</sup> The spectrum of pure Aerosil exhibited an absorption band at about 1100 cm<sup>-1</sup> attributed to Si–O–Si asymmetric stretching vibration, and 810 cm<sup>-1</sup> peak appeared due to the symmetric deformation of the Si–O–Si bond.<sup>24</sup> The –CH stretching was clearly noticed at 2922 cm<sup>-1</sup> for all VAL-containing formulations. The –CH and –NH<sub>2</sub> bendings were ascribed to the comparatively weak absorption around 1465 and 1603 cm<sup>-1</sup>, respectively. The spectra also showed absorption bands at 1639 and 1115 cm<sup>-1</sup>, which were caused by the OH deformational mode of water and the longitudinal Si–O stretching vibration of Aerosil. This indicated that valsartan and Aerosil were present in the film matrix. In the spectra of all formulations, the peaks at 1650 and 1031 cm<sup>-1</sup> were broadened. The high intensity of carboxyl carbonyl peak at 1733 cm<sup>-1</sup> of valsartan became very weak, whereas the amide carbonyl stretching band was recorded at 1650 cm<sup>-1</sup>, a higher wave number than the drug alone in film formulation. The broad band between 3200 to 3500 cm<sup>-1</sup> was attributed to the presence of the O–H stretching frequency of silanol group bonded to the inorganic structure of containing

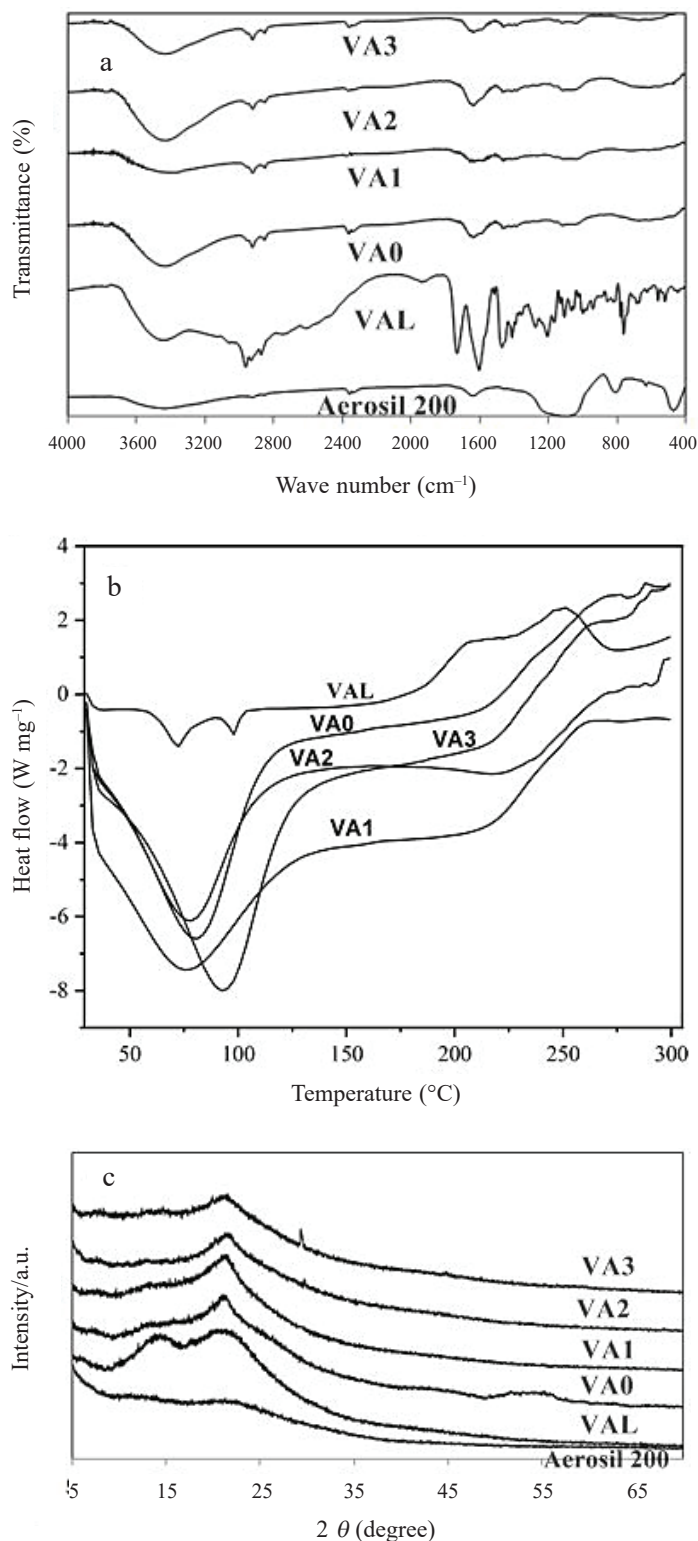


Fig. 1 – FTIR-ATR spectroscopy, DSC curve interpretation, X-ray diffraction of pure valsartan and film formulations

$\text{SiO}_2$ , and hydrogen bonds between adsorbed water and silanol. Aerosil is a proton donor and acceptor due to presence of silanol group on its surface. As a result, drug and Aerosil possibly interact by hydrogen bond formation.<sup>16,25,26</sup>

## DSC

Thermal analysis of pure valsartan and film formulations is presented in Fig. 1b. Valsartan showed two endothermic peaks at 72.12 °C ( $\Delta H=10.84 \text{ J g}^{-1}$ ) and 98.29 °C ( $\Delta H=3.15 \text{ J g}^{-1}$ ), indicating loss of adsorbed water and melting of crystalline drug, respectively.<sup>27,28</sup> An exothermic peak with  $T_{\text{onset}}$  at about 168 °C is associated with the tendency of decomposition.<sup>29</sup> Crystalline nature of pure valsartan has also been supported by the literature reports.<sup>28,30</sup> Disappearance of two endothermic peaks of valsartan indicated the dispersion of valsartan in HPMC-Aerosil matrix, resulting in almost complete amorphisation.<sup>31</sup> Absence of exothermic propensity also indicated the stabilisation of drug in the prepared film formulation. A wide endothermic shouldering in the range of 60–100 °C specified water evaporation of the polymeric matrix film.<sup>32</sup>

## XRD

Characteristic XRD peaks at 13.82° and 22° signified the crystalline nature of pure valsartan.<sup>31</sup> The diffraction pattern of the film formulation revealed no sharp peak, suggesting overall amorphisation of drug in the film (Fig. 1c). This result indicated the presence of drug in dispersed state in the polymer-Aerosil matrix. The diffuse peak observed in the spectra may be due to the porous carrier.<sup>33</sup>

## SEM

Fig. 2 presents the SEM image of pure valsartan, Aerosil, and films with and without Aerosil. The morphology of the pure valsartan showed geometrical slab-like crystal. Aerosil appeared with a rough and porous particle. In the SEM of the film formulations, the drug crystal geometry had almost disappeared, in the presence and absence of the Aerosil particle. Some Aerosil particles are clearly visible in the Aerosil-containing film formulation even under high shear force mixing conditions before casting.<sup>16</sup>

## In vitro drug release study

Fig. 3a shows valsartan dissolution in simulated tear fluid of Aerosil-incorporated HPMC films. We observed about 12 % drug release in the first hour, with 45 % after 8 h only from the film without Aerosil. The studies revealed a noticeable improvement in the release rate from all films containing Aerosil compared to absence of Aerosil in the film. Deposited drug molecules on the surface of the colloidal Aerosil particle probably enhanced the drug release.<sup>34,35</sup> The increased dissolution of cilostazol has been reported in the presence of Aerosil due to

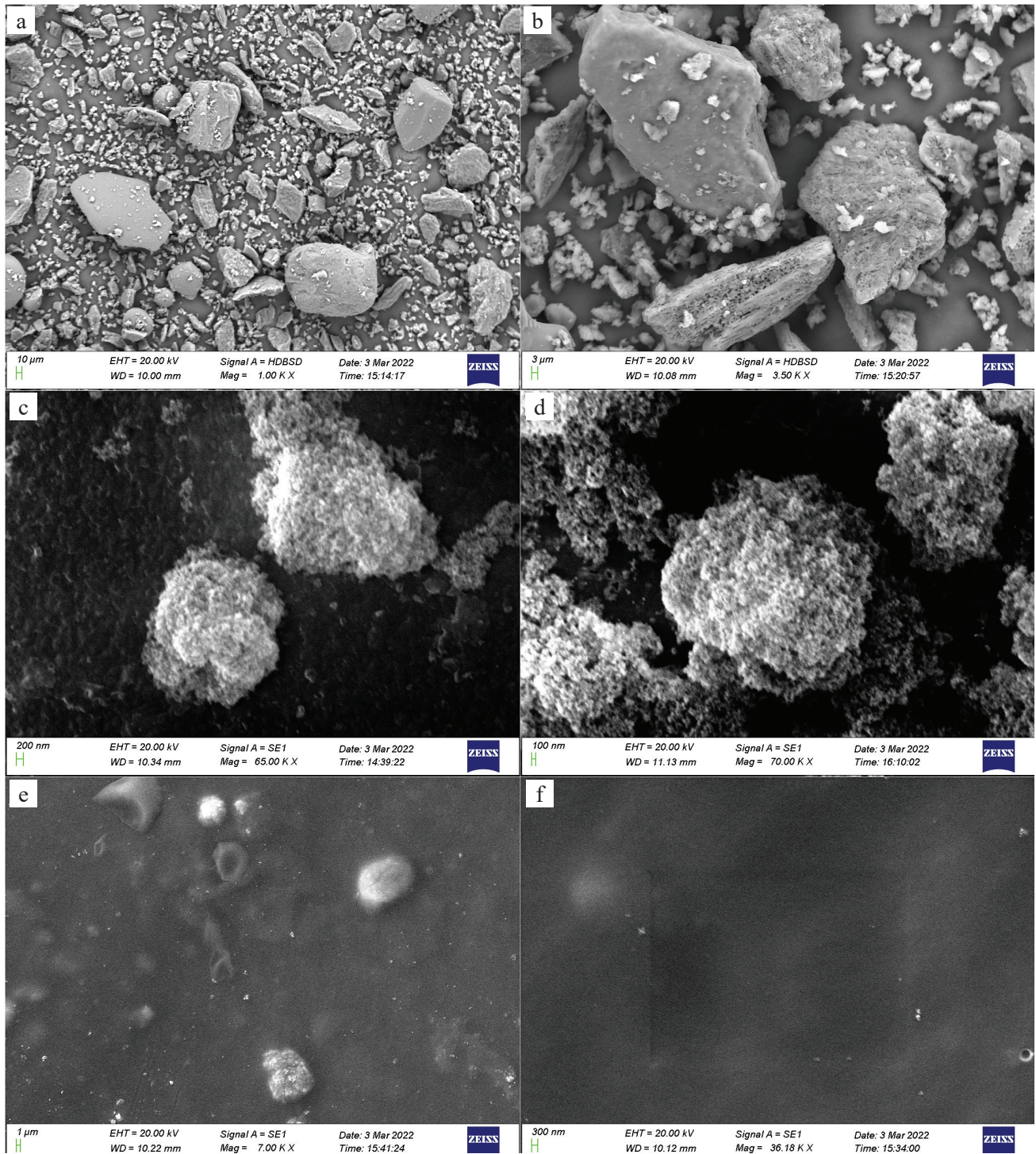


Fig. 2 – SEM image of pure valsartan (a, b), pure Aerosil 200 (c, d), film with Aerosil 200 (VA1) (e), and without Aerosil 200 (VA0) (f)

increased surface area, dispersibility, and wettability of the drug. Drug recrystallisation was prevented due to wide surface area of Aerosil and ensured increased drug release. Aerosil was previously utilised as a carrier to boost the solubility and stability of tadalafil, dutasteride, naftopidil, celecoxib, coenzyme Q10, paclitaxel, due to its wide surface area.<sup>36</sup> Film (VA1) containing highest content of Aerosil showed higher release of about 80 % compared to

other formulations. The following sequence was observed for valsartan release from the HPMC matrix: VA1 > VA2 > VA3 > VA0.

#### Buccal permeation study

Presence of Aerosil significantly improved the mucosal permeation compared to its absence in the film (Fig. 3b). The film VA1 exhibited improved permeation of 10 % in the first hour compared to

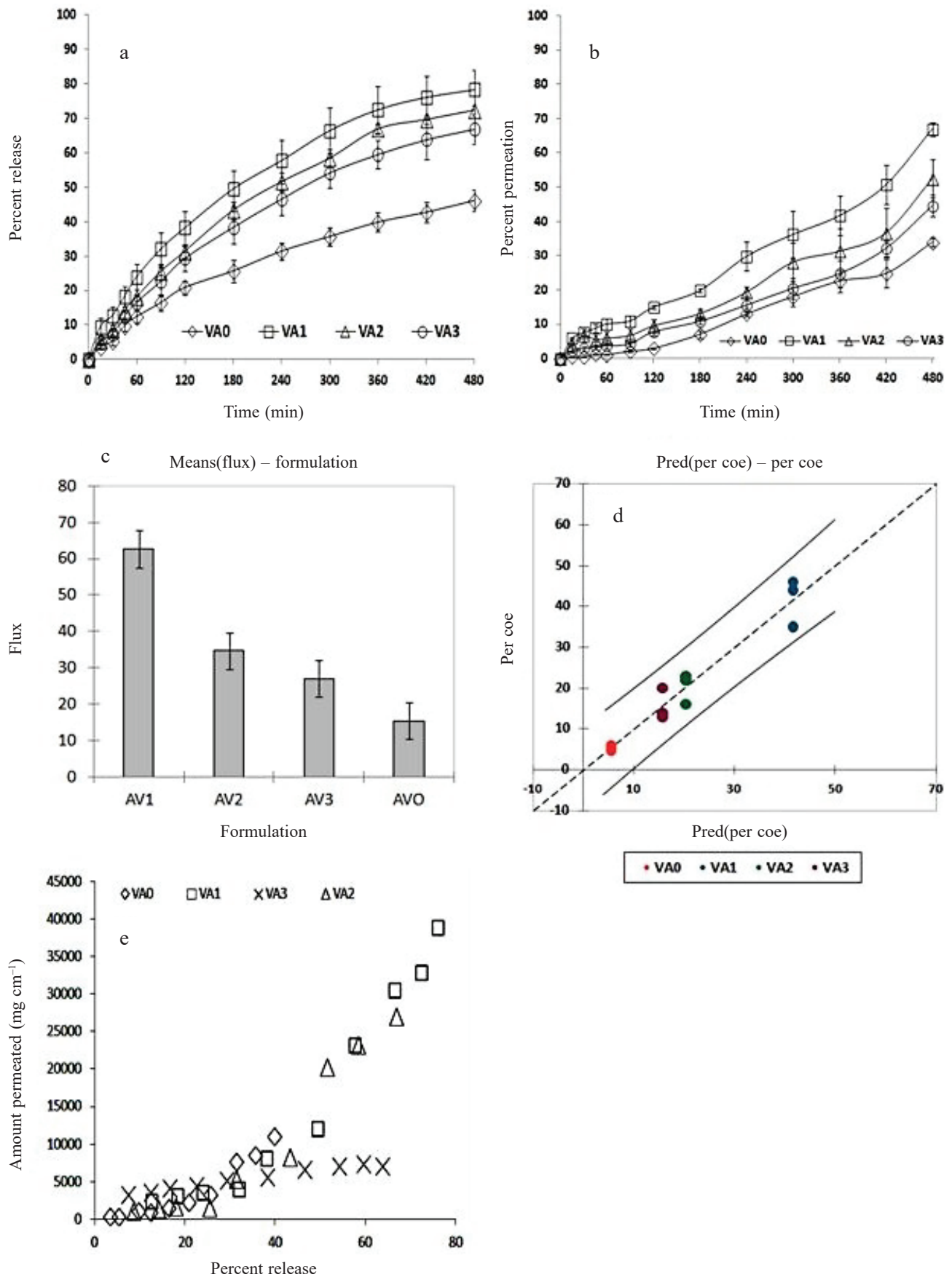


Fig. 3 – *In vitro* dissolution (a), *Ex vivo* buccal permeation (b),  $J_s$  (flux) as a function of Aerosil 200 content (c), mean chart of observation vs. predicted permeation coefficient (d), correlation study between *in vitro* release and *ex vivo* buccal permeation of VAL and film formulations

Table 2 – *In vitro* and *ex vivo* kinetics parameters of valsartan delivery

Film code	<i>In vitro</i> release					<i>Ex vivo</i> permeation					$J_s$ ( $\mu\text{g min}^{-1}$ )	$P_{\text{film}} \cdot 10^{-5}$ ( $\text{cm min}^{-1}$ )
	Peppas		Peppas Sahlin			Peppas		Peppas Sahlin				
	n	$r^2$	$K_1/\text{min}^{-n}$	$K_2/\text{min}^{-2n}$	m	n	$r^2$	$K_1/\text{min}^{-n}$	$K_2/\text{min}^{-2n}$	m		
VA0	0.74	0.983	0.366	0.131	0.578	0.44	0.967	0.357	0.055	0.729	17.2	4.8
VA1	0.57	0.953	0.800	0.404	0.589	0.41	0.961	0.139	0.067	0.756	57.5	46.5
VA2	0.75	0.988	19.2	13.6	0.230	0.41	0.910	0.071	0.015	0.686	35.0	23.5
VA3	0.57	0.989	0.581	0.525	0.526	0.49	0.902	0.104	0.002	0.762	25.3	13.9

Table 3 – Dunnett Test (two-sided)/Analysis of the differences of permeation coefficient between the control group and the other categories with a confidence interval of 95 %

Contrast	Difference	Standardised difference	Critical value	Critical difference	Pr > Diff	Significant
VA0 vs VA1	-36.200	-11.139	2.880	9.359	<0.0001	Yes
VA0 vs VA2	-14.867	-4.574	2.880	9.359	0.005	Yes
VA0 vs VA3	-10.200	-3.139	2.880	9.359	0.034	Yes

only 1 % from VA0 (without Aerosil). Study showed 33 and 67 % permeation after 8 h, respectively. VA1 significantly enhances buccal permeation allowing for the immediate onset of drug action and maintenance of therapeutic level in a controlled manner for the entire duration without reaching toxic drug levels. Permeation of valsartan from the formulation occurred in the following order: VA1 > VA2 > VA3 > VA0.

The *in vitro* and *ex vivo* kinetic parameters of valsartan delivery using Korsmeyer-Peppas and Peppas Sahlin model are given in Table 2. Exponent (n) value of Korsmeyer-Peppas model determines the release and permeation mechanism; n value closer to 0.5 indicates Fickian diffusion, and when  $0.5 < n < 1.0$ , non-Fickian type release is specified.<sup>37</sup> Both the *in vitro* drug release and permeation data fit well with the Korsmeyer-Peppas model ( $r^2 = 0.902-0.989$ ), and the exponent (n) value was found in the range of 0.41–0.75 (> 0.5), indicating that the release and permeation mechanism were mostly diffusion-controlled and partially erosion-controlled.<sup>14,32</sup>

Peppas-Sahlin model was used to estimate the diffusion constant ( $K_1$ ) and chain relaxation constant ( $K_2$ ) in the process of drug release and permeation. The process follows Fickian diffusion if  $K_1 > K_2$ . The process is erosion-based when  $K_2$  is greater than  $k_1$ . If  $K_1 = K_2$ , the process is dependent on both diffusion and erosion.<sup>22</sup> All the drug releases and permeations of the film formulations followed Fickian diffusion ( $K_1 > K_2$ ).<sup>22</sup> Permeation flux ( $J_s$ ) and permeability coefficient ( $P_{\text{film}}$ ) increased with increasing Aerosil concentration in the film formulation from 25.3 to 57.5  $\text{mg min}^{-1}$ , and 13.9 to

46.5  $\text{cm min}^{-1}$ , respectively, compared to the absence of Aerosil (17.2  $\text{mg min}^{-1}$ , and 4.8  $\text{cm min}^{-1}$  respectively) (Fig. 3c). Fig. 3d shows a mean chart of observed vs. predicted permeation coefficients of films, exhibiting the limits of prediction. *In vitro-ex vivo* correlation establishes relationship between drug release and permeation through biological tissue.<sup>38</sup> Drug release is associated with the formulation factors that may affect permeation. An *in vitro-ex vivo* correlation validates the predictability of tissue permeation over the range of *in vitro* release data. A good Level A correlation (1:1 relationship) between *in vitro* release and *ex vivo* permeation at the same time point was established (correlation coefficient 0.900 – 0.974) to ensure batch-to-batch consistency (Fig. 3e). The permeation coefficient of all the formulation differs significantly from the control formulation (VA0) according to Dunnett's test (Table 3). The results revealed that the presence of Aerosil in the buccal film improved the delivery of valsartan and sustained for a period of more than 8 h.

### Molecular docking study

The individual docking score of HPMC-SiO<sub>2</sub>, HPMC-VAL, VAL-SiO<sub>2</sub>, and HPMC-SiO<sub>2</sub>-VAL is presented in Table 4. Binding affinity of HPMC-VAL and VAL-SiO<sub>2</sub> showed docking score of -1.65 and -1.45  $\text{kcal mol}^{-1}$ , respectively. Further, the docking score of ternary binding of HPMC-SiO<sub>2</sub>-VAL showed -2.15  $\text{kcal mol}^{-1}$  through more molecular interactions with different bond lengths (Fig. 4). Overall, the docking analysis validates the possibility of drug delivery, and the fitting of a drug with a stable configuration and favourable binding

Table 4 – Molecular docking study and interaction analysis of HPMC, Aerosil, and valsartan in computational drug analysis prospective

Sl. No.	Interacted molecule	Docking score (kcal mol <sup>-1</sup> )	Interacted atoms	Bond length (Å)
1	HPMC-SiO <sub>2</sub>	-1.41	OH-O (H-bond)	2.96
2	HPMC-VAL	-1.65	C-O, C-N (C-bonds) OH-O (H-bond)	2.38, 2.87, 2.57
3	VAL-SiO <sub>2</sub>	-1.45	OH-O (H-bond)	2.66
4	HPMC-SiO <sub>2</sub> -VAL	-2.15	C-O, C-N (C-bonds) OH-O (H-bond) OH- $\pi$ -orbital (C-bond)	2.38, 2.87, 2.57 3.12

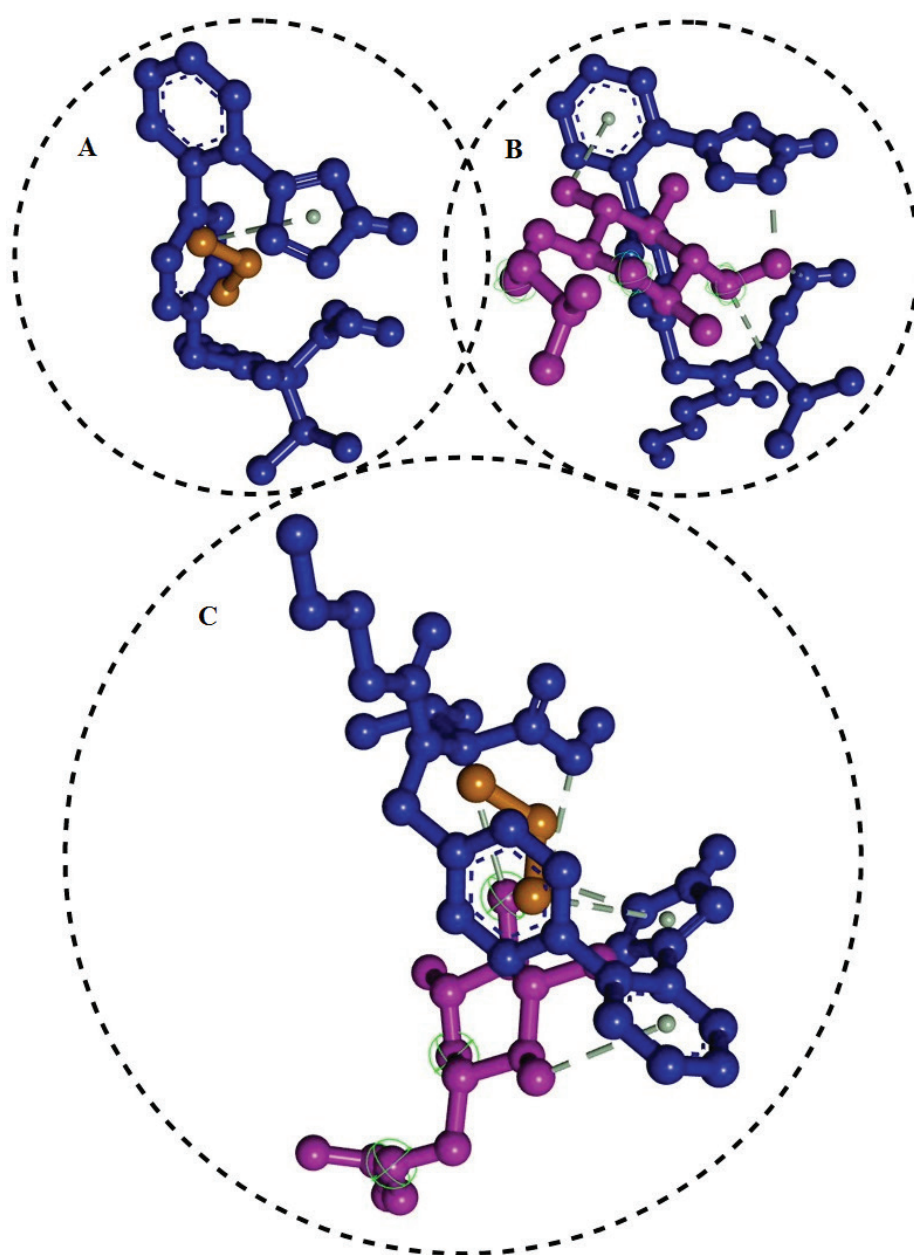


Fig. 4 – Computational study of VAL-Aerosil 200 (a), HPMC-VAL (b), HPMC-VAL-Aerosil 200 (c); where HPMC (dark peach) – VAL (dark blue) – Aerosil 200 (dark yellow)

energy (dipole-dipole interaction, H-bonding, ion-dipole, van der Waals, etc.) in a theoretical drug perspective. There was an ideal interaction between polar organic molecules and the HPMC's hydroxyl groups. According to the experimental section, the adsorption of VAL with HPMC-SiO<sub>2</sub> matrix formulation might have influenced the improved drug release and tissue permeation. Molecular modelling study supports that SiO<sub>2</sub> interactions played a vital role in enhancing the stability and solubility of the complex compared to the absence of SiO<sub>2</sub>.<sup>39</sup> As a result, as predicted by our hypothesis, the computational technique realistically represented the building blocks, binding energy, and molecular interaction as part of early drug development, drug chemistry, and drug delivery analysis.<sup>23,26</sup>

## Conclusion

Colloidal silicon dioxide incorporated valsartan buccal film was prepared successfully for improved and sustained drug delivery. FTIR spectroscopy and DSC thermogram revealed no major drug-carrier interaction. The film showed no intense X-ray diffraction pattern indicating dispersed state of drug in the polymer-Aerosil matrix. The *in vitro* and *ex vivo* permeation data exhibited that the formulation containing the highest amount of Aerosil (VA1) improved release and buccal permeation mostly in a sustained manner compared to the AV0 free of Aerosil to the least. Computational modelling showed a stable configuration with favourable docking score of  $-2.15$  kcal mol<sup>-1</sup> of the Aerosil-incorporated valsartan buccal film in HPMC matrix (HPMC-SiO<sub>2</sub>-VAL). Aerosil-incorporated valsartan film could be used for possible improved and sustained buccal delivery.

## ACKNOWLEDGEMENT

The authors are grateful to the Department of Science & Technology, Ministry of Science & Technology, New Delhi, India, for providing INSPIRE fellowship to Rakesh Swain (IF 180581). The authors are also very grateful to the President, Siksha O Anusandhan (Deemed to be University) for providing other facilities. The authors are also grateful to Novartis (Mumbai, India) for the gift sample of Valsartan.

## FUNDING

Not applicable

## AUTHORS' CONTRIBUTIONS

RS and SM gave a substantial contribution to the design and writing of the manuscript. SN and

PB assisted during the *in vivo*, *ex vivo* studies. SSS designed the molecular docking study. RS prepared the final manuscript which was further reviewed by SM. SM was in charge of the whole operation, rectification, and approval of the manuscript. All authors read and approved the final version of the manuscript.

## References

1. Nekkanti, V., Wang, Z., Betageri, G. V., Pharmacokinetic evaluation of improved oral bioavailability of valsartan: Proliposomes versus self-nanoemulsifying drug delivery system, *AAPS Pharm. Sci. Tech.* **17**(4) (2016) 851. doi: <https://doi.org/10.1208/s12249-015-0388-8>
2. Berkane, N., Carlier, P., Verstraete, L., Mathieu, E., Heim, N., Uzan, S., Fetal toxicity of valsartan and possible reversible adverse side effects, *Birth Defects Res. A Clin. Mol. Teratol.* **70**(8) (2004) 547. doi: <https://doi.org/10.1002/bdra.20047>
3. Chella, N., Shastri, N., Tadikonda, R. R., Use of the liquid compact technique for improvement of the dissolution rate of valsartan, *Acta Pharm. Sin. B* **2**(5) (2012) 502. doi: <https://doi.org/10.1016/j.apsb.2012.07.005>
4. Yeom, D. W., Chae, B. R., Son, H. Y., Kim, J. H., Chae, J. S., Song, S. H., Oh, D., Choi, Y. W., Enhanced oral bioavailability of valsartan using a polymer-based supersaturable self-microemulsifying drug delivery system, *Int. J. Nanomed.* **12** (2017) 3533. doi: <https://doi.org/10.2147/IJN.S136599>
5. Kim, M. S., Baek, I. H., Fabrication and evaluation of valsartan-polymer-surfactant composite nanoparticles by using the supercritical antisolvent process, *Int. J. Nanomed.* **9** (2014) 5167. doi: <https://doi.org/10.2147/IJN.S71891>
6. Yan, Y. D., Sung, J. H., Kim, K. K., Kim, D. W., Kim, J. O., Lee, B. J., Yong, C. S., Choi, H. G., Novel valsartan-loaded solid dispersion with enhanced bioavailability and no crystalline changes, *Int. J. Pharm.* **422**(1-2) (2012) 202. doi: <https://doi.org/10.1016/j.ijpharm.2011.10.053>
7. Dudognon, E., Willart, J. F., Caron, V., Capet, F., Larsson, T., Descamps, M., Formation of budesonide/ $\alpha$ -lactose glass solutions by ball-milling, *Solid State Commun.* **138**(2) (2006) 68. doi: <https://doi.org/10.1016/j.ssc.2006.02.007>
8. Sohail, M., Ahmad, M., Minhas, M. U., Rashid, H., Khalid, I., Development and *in vitro* evaluation of high molecular weight chitosan based polymeric composites for controlled delivery of valsartan, *Adv. Polym. Technol.* **35**(4) (2016) 361. doi: <https://doi.org/10.1002/adv.21558>
9. Vaccaro, L., Vaccaro, G., Agnello, S., Buscarino, G., Cannas, M., Wide range excitation of visible luminescence in nanosilica, *Solid State Commun.* **150**(45-46) (2010) 2278. doi: <https://doi.org/10.1016/j.ssc.2010.09.025>
10. Azarudeen, R. S., Thirumarimurugan, M., Athmiya, K. P., Monisha, R., Prashanthini, V., Antibacterial chitosan-copolymer membranes for drug delivery: Synthesis, characterization, drug release profile and kinetics, *J. Chem. Technol. Biotechnol.* **92**(7) (2017) 1659. doi: <https://doi.org/10.1002/jctb.5162>
11. Harris, D., Robinson, J. R., Drug delivery via the mucous membranes of the oral cavity, *J. Pharm. Sci.* **81**(1) (1992) 10. doi: <https://doi.org/10.1002/jps.2600810102>

12. Lamberti, G., Cascone, S., Titomanlio, G., Barba, A. A., Controlled release of drugs from hydrogel based matrices systems: Experiments and modelling, *Chem. Biochem. Eng. Q.* **26**(4) (2012) 321.  
doi: <https://doi.org/10.15255/CABEQ.2014.108>
13. Karavana, S. Y., Güneri, P., Ertan, G., Benzylamine hydrochloride buccal bioadhesive gels designed for oral ulcers: Preparation, rheological, textural, mucoadhesive and release properties, *Pharm. Dev. Technol.* **14**(6) (2009) 623.  
doi: <https://doi.org/10.3109/10837450902882351>
14. Pattanaik, S., Nandi, S., Swain, R., Sahoo, R. N., Nanda, A., Mallick, S., Effect of quaternary ammonium surfactant on buccal permeation of budesonide film formulation: In silico docking studies, *J. Sci. Ind. Res.* **81**(12) (2022) 1259.  
doi: <https://doi.org/10.56042/jsir.v81i12.61765>
15. Nanda, A., Sahoo, R. N., Pramanik, A., Mohapatra, R., Pradhan, S. K., Thirumurugan, A., Das, D., Mallick, S., Drug-in-mucoadhesive type film for ocular anti-inflammatory potential of amlodipine: Effect of sulphobutyl-ether-beta-cyclodextrin on permeation and molecular docking characterization, *Colloids Surf. B: Biointerfaces.* **172** (2018) 555.  
doi: <https://doi.org/10.1016/j.colsurfb.2018.09.011>
16. Swain, R., Nandi, S., Sahoo, R. N., Swain, S. S., Mohapatra, S., Mallick, S., Bentonite clay incorporated topical film formulation for delivery of trimetazidine: Control of ocular pressure and in vitro-in vivo correlation, *J. Drug Deliv. Sci. Technol.* **67** (2022) 102956.  
doi: <https://doi.org/10.1016/j.jddst.2021.102956>
17. Rawoath, M., Qureshi, D., Hoque, M., Prasad, M. G., Mohanty, B., Alam, M. A., Anis, A., Sarkar, P., Pal, K., Synthesis and characterization of novel tamarind gum and rice bran oil-based emulgels for the ocular delivery of antibiotics, *Int. J. Biol. Macromol.* **164** (2020) 1608.  
doi: <https://doi.org/10.1016/j.ijbiomac.2020.07.231>
18. Das, B., Nayak, A. K., Nanda, U., Topical gels of lidocaine HCl using cashew gum and Carbopol 940: Preparation and in vitro skin permeation, *Int. J. Biol. Macromol.* **62** (2013) 514.  
doi: <https://doi.org/10.1016/j.ijbiomac.2013.09.049>
19. Nanda, A., Das, S., Sahoo, R. N., Nandi, S., Swain, R., Pattanaik, S., Das, D., Mallick, S., Aspirin-hydrogel ocular film for topical delivery and ophthalmic anti-inflammation, *J. Serb. Chem. Soc.* **87**(7-8) (2022) 829.  
doi: <https://doi.org/10.2298/JSC210504019N>
20. Wada, R., Hyon, S. H., Ikada, Y., Kinetics of diffusion-mediated drug release enhanced by matrix degradation, *J. Control Release* **37**(1-2) (1995) 151.  
doi: [https://doi.org/10.1016/0168-3659\(95\)00075-J](https://doi.org/10.1016/0168-3659(95)00075-J)
21. Nandi, S., Ojha, A., Nanda, A., Sahoo, R. N., Swain, R., Pattanaik, K. P., Mallick, S., Vildagliptin plasticized hydrogel film in the control of ocular inflammation after topical application: Study of hydration and erosion behaviour, *Z. Phys. Chem.* **236**(2) (2022) 275.  
doi: <https://doi.org/10.1515/zpch-2021-3081>
22. Moydeen, A. M., Padusha, M. S. A., Thamer, B. M., Ahamed N. A., Al-Enizi, A. M., El-Hamshary, H., El-Newehy, M. H., Single-nozzle core-shell electrospun nanofibers of PVP/dextran as drug delivery system, *Fibers Polym.* **20** (2019) 2078.  
doi: <https://doi.org/10.1007/s12221-019-9187-2>
23. Swain, S. S., Paidesetty, S. K., Dehury, B., Das, M., Vedithi, S. C., Padhy, R. N., Computer-aided synthesis of dapsone-phytochemical conjugates against dapsone-resistant *Mycobacterium leprae*, *Sci. Rep.* **10**(1) (2020) 1.  
doi: <https://doi.org/10.1038/s41598-020-63913-9>
24. Monteiro, M. S. D. S. D. B., Cucinelli Neto, R. P., Santos, I. C. S., Silva, E. O. D., Tavares, M. I. B., Inorganic-organic hybrids based on poly ( $\epsilon$ -Caprolactone) and silica oxide and characterization by relaxometry applying low-field NMR, *Mater. Res.* **15** (2012) 825.  
doi: <https://doi.org/10.1590/S1516-14392012005000121>
25. Shrivastava, A. R., Ursekar, B., Kapadia, C. J., Design, optimization, preparation and evaluation of dispersion granules of valsartan and formulation into tablets, *Curr. Drug Deliv.* **6**(1) (2009) 28.  
doi: <https://doi.org/10.2174/156720109787048258>
26. Sahoo, R. N., Nanda, A., Pramanik, A., Nandi, S., Swain, R., Pradhan, S. K., Mallick, S., Interactions between Ibuprofen and Silicified-MCC: Characterization, drug release and modeling approaches, *Acta Chim. Slov.* **66**(4) (2019) 923.  
doi: <https://doi.org/10.17344/acsi.2019.5139>
27. Medarević, D., Cvijić, S., Dobričić, V., Mitrić, M., Djuriš, J., Ibrić, S., Assessing the potential of solid dispersions to improve dissolution rate and bioavailability of valsartan: In vitro-in silico approach, *Eur. J. Pharm. Sci.* **124** (2018) 188.  
doi: <https://doi.org/10.1016/j.ejps.2018.08.026>
28. Tran, T. T. D., Tran, P. H. L., Park, J. B., Lee, B. J., Effects of solvents and crystallization conditions on the polymorphic behaviors and dissolution rates of valsartan, *Arch. Pharm. Res.* **35** (2012) 1223.  
doi: <https://doi.org/10.1007/s12272-012-0713-7>
29. Júlio, T. A., Zâmara, I. F., Garcia, J. S., Trevisan, M. G., Compatibility and stability of valsartan in a solid pharmaceutical formulation, *Braz. J. Pharm. Sci.* **49** (2013) 645.  
doi: <https://doi.org/10.1590/S1984-82502013000400003>
30. Yan, Y. D., Sung, J. H., Kim, K. K., Kim, D. W., Kim, J. O., Lee, B. J., Yong, C. S., Choi, H. G., Novel valsartan-loaded solid dispersion with enhanced bioavailability and no crystalline changes, *Int. J. Pharm.* **422**(1-2) (2012) 202.  
doi: <https://doi.org/10.1016/j.ijpharm.2011.10.053>
31. Ha, N. S., Tran, T. T. D., Tran, P. H. L., Park, J. B., Lee, B. J., Dissolution-enhancing mechanism of alkalizers in poloxamer-based solid dispersions and physical mixtures containing poorly water-soluble valsartan, *Chem. Pharm. Bull.* **59**(7) (2011) 844.  
doi: <https://doi.org/10.1248/cpb.59.844>
32. Pattanaik, S., Nandi, S., Sahoo, R. N., Nanda, A., Swain, R., Das, S., Mallick, S., Budesonide-cyclodextrin in hydrogel system: Impact of quaternary surfactant on in vitro-in vivo assessment of mucosal drug delivery, *Revista de Chimie* **71** (2020) 332.  
doi: <https://doi.org/10.37358/RC.20.6.8200>
33. Beg, S., Swain, S., Singh, H. P., Patra, C. N., Rao, M. E., Development, optimization, and characterization of solid self-nanoemulsifying drug delivery systems of valsartan using porous carriers, *AAPS PharmSciTech.* **13**(4) (2012) 1416.  
doi: <https://doi.org/10.1208/s12249-012-9865-5>
34. Albertini, B., Passerini, N., González-Rodríguez, M. L., Perissutti, B., Rodríguez, L., Effect of Aerosil® on the properties of lipid controlled release microparticles, *J. Control Release* **100**(2) (2004) 233.  
doi: <https://doi.org/10.1016/j.jconrel.2004.08.013>
35. Hassen, J. H., Silver, J., Chemisorption role of clay surfaces in the synthesis of porphyrins from its raw materials via room temperature reactions, *Chem. Biochem. Eng. Q.* **36**(1) (2022) 17.  
doi: <https://doi.org/10.15255/CABEQ.2021.2001>

36. Choi, J. S., Kwon, S. H., Lee, S. E., Jang, W. S., Byeon, J. C., Jeong, H. M., Park, J. S., Use of acidifier and solubilizer in tadalafil solid dispersion to enhance the in vitro dissolution and oral bioavailability in rats, *Int. J. Pharm.* **526**(1-2) (2017) 77.  
doi: <https://doi.org/10.1016/j.ijpharm.2017.04.056>
37. Tighsazzadeh, M., Mitchell, J. C., Boateng, J. S., Development and evaluation of performance characteristics of timolol-loaded composite ocular films as potential delivery platforms for treatment of glaucoma, *Int. J. Pharm.* **566** (2019) 111.  
doi: <https://doi.org/10.1016/j.ijpharm.2019.05.059>
38. Bao, Q., Newman, B., Wang, Y., Choi, S., Burgess, D. J., In vitro and ex vivo correlation of drug release from ophthalmic ointments, *J. Control Release* **276** (2018) 93.  
doi: <https://doi.org/10.1016/j.jconrel.2018.03.003>
39. Suvarna, V., Kajwe, A., Murahari, M., Pujar, G. V., Inturi, B. K., Sherje, A. P., Inclusion complexes of Nateglinide with HP- $\beta$ -CD and L-arginine for solubility and dissolution enhancement: Preparation, characterization, and molecular docking study, *J. Pharm. Innov.* **12** (2017) 168.  
doi: <https://doi.org/10.1007/s12247-017-9275-z>